

Comparison and Relation between Crystal Structures and Magnetic Properties of Two Manganese(II) Coordination Polymers Based on (Triazol-1-yl)iso/terephthalic Acid^①

YAN Juan-Zhi^a ZHAO Dan^a LU Li-Ping^{b②}

^a (Taiyuan University, Taiyuan 030032, China)

^b (Institute of Molecular Science, Shanxi University, Taiyuan 030006, China)

ABSTRACT One new Mn(II) coordination polymer, $[\text{Mn}(\text{Htia})_2(\text{H}_2\text{O})_2]_n \cdot 2\text{nH}_2\text{O}$ (**1**, H_2tia = 4-(1,2,4-triazol-1-yl)isophthalic acid) has been synthesized in mixed solvents under solvothermal conditions. Further characterizations including single-crystal XRD, elemental analysis, IR spectroscopy, thermogravimetric analysis and powder XRD were performed to verify the structure. Complex **1** displays a one-dimensional (1D) chain and is similar to a reported Mn(II) complex **2** $\{[\text{Mn}(\text{Htta})_2(\text{H}_2\text{O})_2] \cdot 2\text{H}_2\text{O}\}_n$. It crystallizes in triclinic $P\bar{1}$ space group, with $a = 7.5557(3)$, $b = 7.5974(3)$, $c = 11.8448(4)$ Å, $\alpha = 90.088(1)^\circ$, $\beta = 95.863(1)^\circ$, $\gamma = 113.668(1)^\circ$, $V = 618.81(4)$ Å³, $Z = 1$, $M_r = 591.36$ g/mol, $D_c = 1.587$ mg/m³, $\mu = 0.609$ mm⁻¹, $F(000) = 303$, $GOOF = 1.062$, the final $R = 0.0359$ and $wR = 0.0818$ for 4272 observed reflections with $I > 2\sigma(I)$. Based on two similar structures, Hirshfeld surface analysis confirmed both structures are mainly stabilized by $\text{O} \cdots \text{H}/\text{H} \cdots \text{O}$ and $\text{C} \cdots \text{H}/\text{H} \cdots \text{C}$ hydrogen bonds. Further, weak ferromagnetic behaviors between adjacent Mn(II) ions in 1D chain are obtained.

Keywords: manganese(II) complexes, (triazol-1-yl)iso/terephthalic acid, crystal structure, Hirshfeld surface, magnetic properties; DOI: 10.14102/j.cnki.0254-5861.2011-3186

1 INTRODUCTION

The inorganic-organic complexes with peculiar structures and potential applications have attracted much attention and seen great progress in recent years^[1-3]. Especially in the field of magnetism, many manganese coordination polymers have been designed and synthesized^[4,5]. The key to designing such material is to select a bridging ligand that can effectively construct novel structures and mediate the magnetic coupling^[6,7]. Carboxylate groups are among the most extensively investigated bridges due to their various bridging modes such as *syn-syn*, *syn-anti*, and *anti-anti*^[8,9], which can easily form extended coordination networks with diverse topologies, and efficiently mediate either ferromagnetic (FM) or antiferromagnetic (AFM) coupling^[10]. The polycarboxylate ligands that contain multiple bridging moieties and multidentate chelating modes are one of the most widely used linkers in the design of polynuclear complexes with interesting magnetic properties. It is well-known that substituted 1,2,4-triazoles are widely used to construct novel

MOFs due to their versatile coordination modes^[11-13]. Specific structure could regulate magnetism behavior to realize the functionalization of the structure. In our previous work, several 1,2,4-triazole complexes have been reported^[14-17], where manganese complexes^[15] also showed different crystal structures and magnetic properties.

As continuation of our investigation of asymmetrically substituted 1,2,4-triazoles, herein, synthesis and characterization of one new manganese complex based on a bifunctional ligand 4-(1,2,4-triazol-1-yl)isophthalic acid (H_2tia) are presented. We also compared a similar structural complex **2** $\{[\text{Mn}(\text{Htta})_2(\text{H}_2\text{O})_2] \cdot 2\text{H}_2\text{O}\}_n$ ^[18] reported in previous literature based on 2-(1,2,4-triazol-1-yl)terephthalic acid (H_2tta) with the title complex **1**. Ligands H_2tia and H_2tta used are just different in the positions (para-/meta-) of one carboxyl group bonded with benzene ring. For structural investigation and comparison, Hirshfeld surface analysis may better find similarities and minor differences. Magnetic properties of two manganese complexes are described according to structural features in 300~2.0 K.

Received 19 March 2021; accepted 1 June 2021 (CCDC 2034131)

① Supported by the NNSFC (No. 21571118)

② Corresponding author. Professor, majoring in coordination chemistry. E-mail: luliping@sxu.edu.cn

2 EXPERIMENTAL

2.1 Materials and methods

All reagents were purchased commercially and used without further purification. Elemental analyses (C, H, and N) were performed on an Elementar Vario EL III analyzer. FT-IR spectra were recorded from KBr pellets in the range of 4000~400 cm^{-1} on a Bruker TENSOR27 Spectrometer. Powder X-ray diffraction (PXRD) data were collected on a Rikagu Smartlab X-ray diffractometer with Cu- $K\alpha$ radiation ($\lambda = 1.5406 \text{ \AA}$) in the 2θ range of $5\sim 50^\circ$ at a rate of $5^\circ/\text{min}$. Thermogravimetric (TG) study was carried out on a Dupont thermal analyzer under 20 mL/min flowing N_2 while ramping the temperature at a rate of 10 K/min from 313 to 1073 K. Variable temperature (2.0~300 K) magnetic susceptibilities of crystalline samples of the complexes were measured on a Quantum Design MPMS SQUID magnetometer with an applied field of 1000 Oe.

2.2 Synthesis of complex $[\text{Mn}(\text{Htia})(\text{H}_2\text{O})_2]_n \cdot 2n\text{H}_2\text{O}$ (1)

A mixture of $\text{MnCl}_2 \cdot 4\text{H}_2\text{O}$ (0.0396 g, 0.2 mmol), H_2tia (0.0233 g, 0.1 mmol), CH_3CN (1.0 mL) and H_2O (2.0 mL) was stirred at room temperature, then sealed in a 23.0 mL Teflon-lined stainless-steel vessel, heated at 393 K for 3 days, and cooled to room temperature, obtaining colourless crystals in 46.8% yield (based on Mn(II)). Anal. Calcd. $\text{C}_{20}\text{H}_{20}\text{MnN}_6\text{O}_{12}$ (%): C, 40.62; H, 3.41; N, 14.21. Found (%): C, 39.78; H, 3.44; N, 14.52%. IR (cm^{-1}): 3411 (s), 3137(m),

1957 (w), 1691 (m), 1603 (s), 1510 (s), 1424 (m), 1379 (s), 1300 (s), 1257 (m), 1129 (m), 1106 (m), 1041 (m), 977 (s), 982 (w), 912 (m), 883 (m), 868 (w), 846 (w), 819 (w), 767 (s).

2.3 Synthesis of reported complex

$[\text{Mn}(\text{Htta})(\text{H}_2\text{O})_2]_n \cdot 2n\text{H}_2\text{O}$ (2)

The synthesis of **2** was similar to that of **1** except H_2tia was replaced by H_2tta (0.0233 g, 0.1 mmol). Colourless crystals **2** were obtained in 57.6% yield (based on Mn(II)). The synthesis condition is quite different from the reported method^[18]. Even with different temperature, solvents and metal/ligand ratios, the same structure is obtained, which may display the most stable state in kinetics and thermodynamics system.

2.4 X-ray crystallography

Single-crystal X-ray diffraction data for complex were collected on a Bruker D8 venture diffractometer equipped with graphite-monochromatic Mo $K\alpha$ radiation ($\lambda = 0.71073 \text{ \AA}$) at 298(2) K. Cell parameter was determined using SMART software. Absorption correction was made *via* SADABS program^[19]. The structure was solved by direct methods employed in the SHELXS-2014 program and refined by full-matrix least-squares methods against F^2 with SHELXL-2014^[20]. After all non-H atoms were refined anisotropically, hydrogen atoms attached to carbon atoms were placed geometrically and refined using a riding model approximation. Selected bond lengths, angles and H-bonds are shown in Tables 1 and 2.

Table 1. Selected Bond Lengths (\AA) and Bond Angles ($^\circ$) of Complex 1

Bond	Dist	Bond	Dist	Bond	Dist
Mn(1)–O(5)	2.157(1)	Mn(1)–O(5 ⁱ)	2.157(1)	Mn(1)–O(3 ⁱ)	2.182(1)
Mn(1)–O(3)	2.182(1)	Mn(1)–N(3 ⁱⁱ)	2.264(1)	Mn(1)–N(3 ⁱⁱⁱ)	2.264(1)
Angle	($^\circ$)	Angle	($^\circ$)	Angle	($^\circ$)
O(5)–Mn(1)–O(5 ⁱ)	180.0	O(5)–Mn(1)–O(3 ⁱ)	94.61(4)	O(5 ⁱ)–Mn(1)–O(3 ⁱ)	85.40(4)
O(5)–Mn(1)–O(3)	85.40(4)	O(5 ⁱ)–Mn(1)–O(3)	94.60(4)	O(3 ⁱ)–Mn(1)–O(3)	180.0
O(5)–Mn(1)–N(3 ⁱⁱ)	90.10(5)	O(5 ⁱ)–Mn(1)–N(3 ⁱⁱ)	89.90(5)	O(3 ⁱ)–Mn(1)–N(3 ⁱⁱ)	85.16(4)
O(3)–Mn(1)–N(3 ⁱⁱ)	94.84(4)	O(5)–Mn(1)–N(3 ⁱⁱⁱ)	89.90(5)	O(5 ⁱ)–Mn(1)–N(3 ⁱⁱⁱ)	90.10(5)
O(3 ⁱ)–Mn(1)–N(3 ⁱⁱⁱ)	94.84(4)	O(3)–Mn(1)–N(3 ⁱⁱⁱ)	85.16(4)	N(3 ⁱⁱ)–Mn(1)–N(3 ⁱⁱⁱ)	180.1(0)

Symmetry codes 1: ⁱ $-x, -y + 1, -z + 1$; ⁱⁱ $-x, -y, -z + 1$; ⁱⁱⁱ $x, y + 1, z$; ^{iv} $x, y - 1, z$

Table 2. Hydrogen Bond Geometry (\AA , $^\circ$) for 1

D–H \cdots A	D–H	H \cdots A	D \cdots A	$\angle \text{D–H} \cdots \text{A}$
O(6)–H(6A) \cdots O(3 ^v)	0.82	1.91	2.732(1)	179
O(6)–H(6B) \cdots N(2)	0.82	2.06	2.876(1)	176
O(5)–H(5B) \cdots O(4 ^{vi})	0.81	2.02	2.834(1)	174
O(5)–H(5A) \cdots O(2 ^{vii})	0.84	1.90	2.730(1)	166
O(1)–H(1) \cdots O(6 ^{viii})	0.82	1.76	2.582(1)	174
C(10)–H(10) \cdots O(4 ^{ix})	0.93	2.56	3.465(1)	164
C(7)–H(7) \cdots O(1 ^{iv})	0.93	2.53	3.412(1)	158

Symmetry codes: 1: ^{iv} $x, y - 1, z$; ^v $x + 1, y, z$; ^{vi} $x - 1, y, z$; ^{vii} $-x, -y + 1, -z$; ^{viii} $-x + 1, -y + 1, -z$; ^{ix} $-x + 1, -y, -z + 1$

2.5 Hirshfeld surface (HS) calculations

Molecular Hirshfeld surface calculations were performed by using the CrystalExplorer software ver. 3.1^[21]. Molecular Hirshfeld surfaces are shown as transparent to allow visualization of the molecular and connection environment in crystals. When the cif files of structures **1** and **2** were read into the CrystalExplorer program for analysis, all bond lengths to hydrogen were automatically modified to typical standard neutron values. The 2D fingerprint plots were displayed by using the standard 0.5~2.5 Å view with the d_e and d_i distance scales displayed on the graph axes.

3 RESULTS AND DISCUSSION

3.1 Structural description

X-ray crystallographic analysis reveals complex **1** crystallizes in triclinic system with space group of $P\bar{1}$. As shown in Fig. 1, the Mn(II) coordination consists of four O atoms (O(3), O(3ⁱ), O(5), O(5ⁱ)) in the equatorial plane and two triazolyl axial N (N(3ⁱⁱ), N(3ⁱⁱⁱ)) atoms. The connectivity of **1** is comparable to **2** $\{[\text{Mn}(\text{Htta})_2(\text{H}_2\text{O})_2] \cdot 2\text{H}_2\text{O}\}_n$ ^[18], which is based on a meta-substituted triazolyl carboxylic acid H₂tta similar to H₂tia ligand. H₂tia still keeps one protonated

carboxyl group because no base was introduced, which makes complex **1** the same coordination mode with literature. Central Mn(II) falling in symmetrical center makes each Mn(II) ion joined by double ligands to result in the Mn₂(Htia)₂ 18-membered cycle with a diameter approximately 7.60 and 8.30 Å in **1** (7.15 and 8.83 Å in **2**), and afford a 1D chain along the *b* direction. As shown in Fig. 2, two strands of ligands are held together by Mn(II) atoms and wrapped around each other to form a double chain with Mn··Mn distances of 7.5974(3) Å in **1** (7.1565(2) Å in **2**). Even though the Mn··Mn distance is long, it still leads to weak magnetic interactions, as analyzed in the magnetic part of this context. In addition, there are two intramolecular hydrogen bonds (C–H··O) (Table 2) to stabilize the structure, and the other ones (O–H··O) from coordinated and free water molecules connect primarily the adjacent 1D double chains to form a 3D structure. Interestingly, the distance between pairs of benzene planes of two Htia[−] groups in the 3D supramolecular network of **1** is 4.266 Å (Fig. 2), which is longer than 3.267 Å in complex **2**, which may be attributed to the different dihedral angle between the triazole and benzene rings due to the steric hindrance of para-/metacarboxyl group in the ligand.

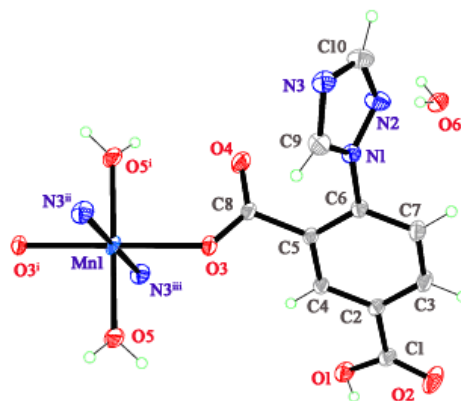


Fig. 1. View of the structure of **1** with 30% thermal ellipsoids
(Symmetry codes: ⁱ $-x, -y + 1, -z + 1$; ⁱⁱ $-x, -y, -z + 1$; ⁱⁱⁱ $x, y + 1, z$)

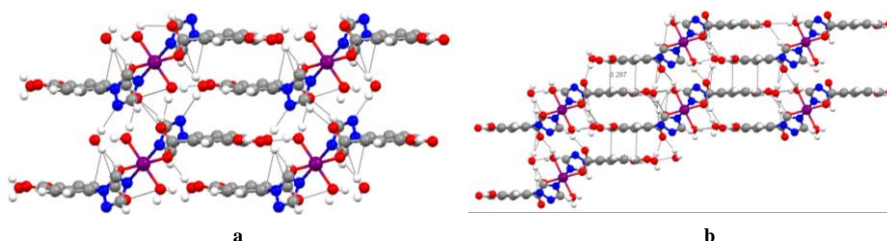


Fig. 2. View of the 3D structures of **1**(a) and **2**(b) through weak interactions

Compared with complex **2** that has been reported^[18], similar 1D chain structures are observed as expected due to

the same coordination sites of two similar partially deprotonated ligands. But different bond distances and bond

angles around the centre metal promote two different octahedra with varying degrees of distortion. For example, the Mn–O bond lengths on the equatorial plane is 2.157(1) and 2.182(1) Å (2.1605(16) and 2.224(2) Å reported in **2**), and the axial Mn–N of 2.264(1) Å in **1** is comparable with 2.260(2) Å in **2**. But all the parameters including bond distances and bond angles are within a reasonable range and match the values reported for similar coordination Mn(II) complexes^[15, 22–24]. Unlike **2** {[Mn(Htta)₂(H₂O)₂] 2H₂O}_n, uncoordinated para-substituted carboxylate group will generate smaller steric hindrance in Htta, displaying a smaller dihedral angle between the triazole ring and benzene ring, which will be reflected on H bonding or $\pi \cdots \pi$ interactions.

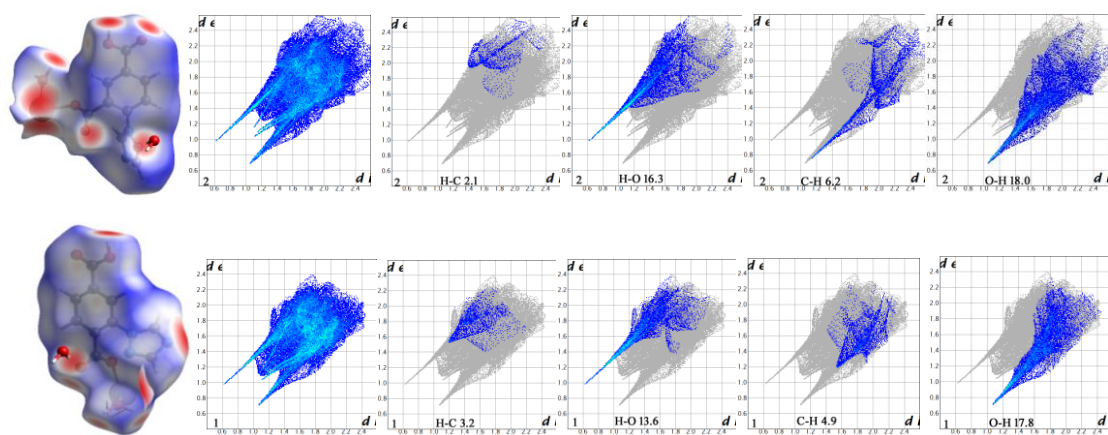


Fig. 3. HS of INDP mapped with d_{norm} (left) and Fingerprint plots (right) (the semitransparent surface shows the enclosed molecule)

In complex **1**, the proportions of H \cdots O/O \cdots H contacts are 16.3 and 18.0% derived from solvent water molecules and carboxyl groups. The proportions of C \cdots H/H \cdots C interactions comprise 2.1 and 6.2% of entire HS surfaces for each molecule. Finally, supramolecular self-assembly and stabilization are derived from those H bonding contacts. Similarly, the contributions C \cdots H/H \cdots C interactions in **2** are 3.2 and 4.9% and the H \cdots O/O \cdots H contacts comprise 13.6 and 17.8%. The HS analysis shows both structures are stabilized mainly by O \cdots H/H \cdots O and C \cdots H/H \cdots C hydrogen bonds. Furthermore, compared with **2**, the O \cdots H/H \cdots O contacts of **1** are slightly increased ($\sim 2\%$) due to the uncoordinated para-/metacarboxyl group. Minor structural changes generate slightly different weak interactions. The fact is indeed different O–H \cdots O bonding between H₂O and carboxylate oxygen. We can see free water molecules are located quite differently. Thus, the Hirshfeld surface analysis could analyze and get insight into weak interactions in the self-assembly system.

3.3 PXRD and thermogravimetric analysis

3.2 Molecular Hirshfeld surface (HS) study

The HS maps of the structures are illustrated in Fig. 3, showing the surfaces are mapped over a d_{norm} ^[25]. The spots especially shaped large deep red depressions on the d_{norm} surfaces, reflecting the effective and strong hydrogen bonding contacts. Light red spots may be indicative of comparable weak C \cdots H contacts. The leading interactions are also visible in the fingerprint plots, which can be decomposed into diverse interaction types to highlight particular atom-pair close contacts. In the fingerprint plots, $d_e > d_i$ represents that the molecule could be the donor, otherwise an acceptor should be $d_e > d_i$.

The experimental and simulated PXRD patterns of complexes **1** and **2** are shown in Fig. 4. The experimental PXRD pattern of the bulk product is in good agreement with the calculated XRD pattern from single-crystal X-ray diffraction results.

As illustrated in Fig. 5, complex **1** has similar thermogravimetric plot with that of **2** {[Mn(Htta)₂(H₂O)₂] 2H₂O}_n^[18], which matches well with their structural composition. The first weight-loss stage occurred about 361–450 K without any loss below 361 K, corresponding to the loss of four water molecules, including coordinated and lattice ones (expt. 12.7%, calcd. 12.2%). The dehydrated complex then decomposes roughly at 548 K as indicated by the huge weight loss in the TG curve.

3.4 Magnetic properties

Mn(II) ions endowed with d^5 electronic configuration could induce paramagnetic behavior in a magnetic field. As expected, the magnetic behaviors of **1** and **2** were successfully recorded and shown as χ_M^{-1} and $\chi_M T$ versus T plots with extremely similar trends in Fig. 6.

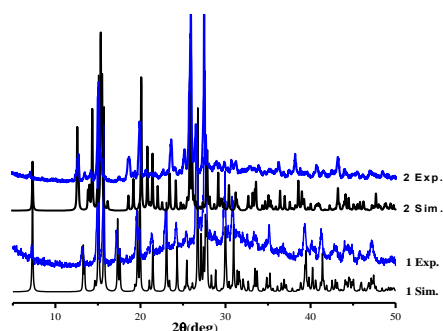


Fig. 4. PXRD patterns for samples 1 and 2

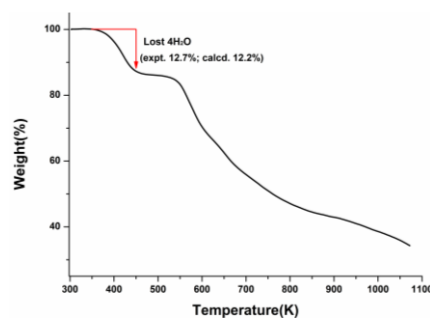
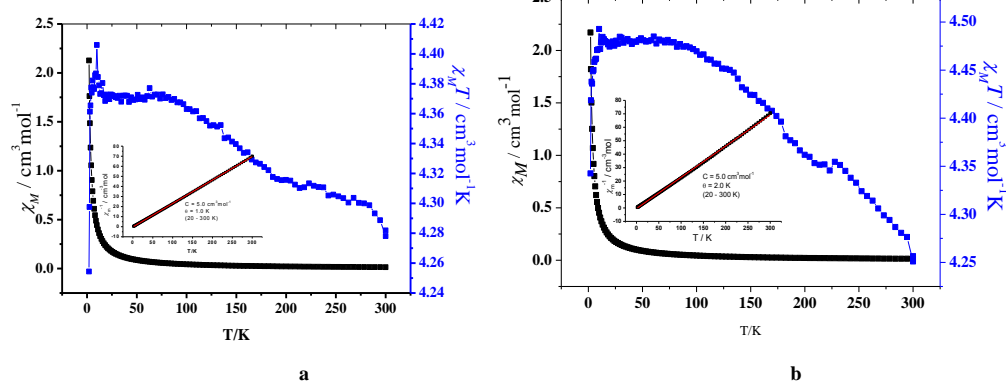


Fig. 5. TG plot of complex 1

Fig. 6. Plots of $\chi_M T$ and χ_M vs. T for 1 (a) and 2 (b) (Inset: plot of χ_M^{-1} vs. T)

The experimental $\chi_M T$ values of **1** and **2** at room temperature are 4.28 and 4.25 $\text{cm}^3 \text{K mol}^{-1}$, which are slightly lower than 4.75 $\text{cm}^3 \cdot \text{K mol}^{-1}$ of one uncorrelated theoretical spin value (Mn(II): $S = 5/2$, $g = 2.0$). Upon cooling, the $\chi_M T$ values steadily increase up to 4.4 $\text{cm}^3 \text{K mol}^{-1}$ for **1** and 4.5 $\text{cm}^3 \text{K mol}^{-1}$ for **2** from room temperature to 10.0 K, and then the values rapidly decrease down to 4.25 $\text{cm}^3 \text{K mol}^{-1}$ for **1** and 4.3 $\text{cm}^3 \text{K mol}^{-1}$ for **2** at 2.0 K. Gradually monotonically increasing trends reflect the ferromagnetic behavior between 300 and 10 K. While, the rapid decrease of $\chi_M T$ to 4.25 $\text{cm}^3 \text{K mol}^{-1}$ for **1** and 4.3 $\text{cm}^3 \text{K mol}^{-1}$ for **2** between 10 and 2.0 K is probably caused by weak intermolecular antiferromagnetic interactions and zero-Feld splitting. The data in the temperature range of 2.0~300 K obey the Curie-Weiss law $\chi = C/(T - \theta)$ with $C = 2.0$ (**1**) and 1.0 (**2**) $\text{cm}^3 \text{K mol}^{-1}$ and $\theta = 4.0$ (**1**) and 2.0 (**2**) K. The positive θ values are indicative of similar weak ferromagnetic interactions between adjacent Mn(II) ions in the network structure of complexes. By magnetic structure analysis, the observed weak magnetic behavior can be interpreted in the context of the structures:

large organic linker may be the dominant pathway for magnetic exchange, the longer distance of Mn··Mn will contribute to weaker magnetic interactions. Above extremely similar magnetism indicate Mn··Mn distance and deliver linker are structurally similar.

4 CONCLUSION

In summary, two similar Mn(II) complexes have been synthesized under solvothermal conditions. Their structures and magnetic performances are comparable due to similar organic linkers (H₂tia and H₂tta). Both complexes have a 1D chain arrangement with a mononuclear Mn(II) geometry. The Hirshfeld surfaces analysis shows both structures are stabilized mainly by O··H/H··O and C··H/H··C hydrogen bonds. Both complexes display weak ferromagnetic exchange, which is also comparable with their structures. Thus similar coordination and connection could rarely affect the performance.

REFERENCES

- (1) Lada, Z. G.; Andrikopoulos, K. S.; Chrissanthopoulos, A.; Perlepes, S. P.; Voyiatzis, G. A. A known iron(II) complex in different nanosized particles: variable-temperature Raman study of its spin-crossover behavior. *Inorg. Chem.* **2019**, 58, 5183–5195.
- (2) Zhao, X. X.; Zhang, S. W.; Yan, J. Q.; Li, L. D.; Wu, G. J.; Shi, W.; Yang G. M.; Guan, N. J.; Cheng P. Polyoxometalate-based metal-organic

- frameworks as visible-light-induced photocatalysts. *Inorg. Chem.* **2018**, 57, 5030–5037.
- (3) Zhao, D.; Liu, X. H.; Guo, J. H.; Xu, H. J.; Zhao, Y.; Lu, Y.; Sun, W. Y. Porous metal-organic frameworks with chelating multiamine sites for selective adsorption and chemical conversion of carbon dioxide. *Inorg. Chem.* **2018**, 57, 2695–2704.
- (4) Naiya, S.; Biswas, S.; Drew, M. G. B.; Gómez-García, C. J.; Ghosh, A. A ferromagnetic methoxido-bridged Mn(III) dimer and a spin-canted metamagnetic $\mu_{1,3}$ -azido-bridged chain. *Inorg. Chem.* **2012**, 51, 5332–5341.
- (5) Li, S. D.; Lu, L. P.; Zhu, M. L.; Feng, S. S.; Su, F.; Zhao, X. Exploring the syntheses, structures, topologies, luminescence sensing and magnetism of Zn(II) and Mn(II) coordination polymers based on a semirigid tricarboxylate ligand. *CrystEngComm.* **2018**, 20, 5442–5456.
- (6) Wang, Y. Q.; Jia, Q. X.; Wang, K.; Cheng, A. L.; Gao, E. Q. Diverse manganese(II) coordination polymers with mixed azide and zwitterionic dicarboxylate ligands: structure and magnetic properties. *Inorg. Chem.* **2010**, 49, 1551–1560.
- (7) Dong, X. Y.; Si, C. D.; Fan, Y.; Hu, D. C.; Yao, X. Q.; Yang, Y. X.; Liu, J. C. Effect of N-donor ligands and metal ions on the coordination polymers based on a semirigid carboxylic acid ligand: structures analysis, magnetic properties, and photoluminescence. *Cryst. Growth Des.* **2016**, 16, 2062–2073.
- (8) Su, F.; Lu, L. P.; Feng, S. S.; Zhu, M. L.; Gao, Z.; Dong, Y. Synthesis, structures and magnetic properties in 3D-electron-rich isostructural complexes based on chains with sole syn-anti carboxylate bridges. *Dalton Trans.* **2015**, 44, 7213–7222.
- (9) Li, W.; Jia, H. P.; Ju, Z. F.; Zhang, J. A series of manganese-carboxylate coordination polymers exhibiting diverse magnetic properties. *Dalton Trans.* **2008**, 5350–5357.
- (10) Feng, S. S.; Xie, L.; Lu, L. P.; Zhu, M. L.; Su, F. The diversity of five metal-organic complexes based on an unsymmetrical biphenyl tetracarboxylate: synthesis, structures, magnetism and luminescence. *J. Solid State Chem.* **2018**, 258, 335–345.
- (11) Yang, Y.; Yang, J.; Du, P.; Liu, Y. Y.; Ma, J. F. A series of coordination polymers constructed by the semi-rigid bifunctional ligand 5-((1H-1,2,4-triazol-1-yl)methoxy) isophthalic acid: syntheses, structures and the role of solvents. *CrystEngComm.* **2014**, 16, 1136–1148.
- (12) Xu, Q. W.; Wang, Q. S.; Li, S. S.; Li, X. Cu(II)/Ni(II)-organic frameworks constructed from the homometallic clusters by 5-(2-carboxyphenoxy) isophthalic acid and N-ligand: synthesis, structures and visible light-driven photocatalytic properties. *RSC Adv.* **2019**, 9, 16305–16312.
- (13) Shi, X. J.; Chen, P. Y.; Yin, Z. M.; Li, T.; Wu, M. Z.; Tian, L. Transition metal coordination networks based on 1,3-bis(1,2,4-triazol-1-yl)benzene and isophthalic acid: luminescence and magnetic properties. *Polyhedron* **2018**, 141, 87–93.
- (14) Yan, J. Z.; Lu, L. P. Crystal structure and theoretical studies of tetrahydrate(1-H-1,2,4-triazole-3,5-dicarboxylic acid)nickel. *Chin. J. Struct. Chem.* **2017**, 36, 1334–1340.
- (15) Yan, J. Z.; Lu, L. P.; Zhu, M. L.; Feng, S. S. Self-assembly of novel manganese(II) compounds based on bifunctional-group ligands: synthesis, structures, and magnetic properties. *J. Solid State Chem.* **2018**, 262, 351–359.
- (16) Yan, J. Z.; Lu, L. P. Synthesis, crystal structure and photoluminescence of two new Cu_4I_4 coordination polymers based on 3,5-alkyl-4-amino-1,2,4-triazole. *Chin. J. Inorg. Chem.* **2017**, 33, 1697–1704.
- (17) Yan, J. Z.; Lu, L. P.; Zhu, M. L.; Feng, S. S. Synthesis and structure of a ladder-like co-crystal $\text{Cu}^{\text{I}}\text{Cl}$ with 3,5-dipropyl-4-amino-1,2,4-triazole. *Chin. J. Struct. Chem.* **2015**, 34, 401–407.
- (18) Wang, D. W.; Wang, T.; Yan, T.; Du, L.; Zhao, Q. H. Crystal structure, spectroscopic and thermal properties of copper(II) and manganese(II) coordination polymers based on triazole-benzoic acid ligands. *Transit. Met. Chem.* **2018**, 43, 1–8.
- (19) Sheldrick, G. M. A short history of SHELX. *Acta. Crystallogr.* **2008**, A64, 112–122.
- (20) Sheldrick, G. M. Crystal structure refinement with SHELXL. *Acta. Crystallogr.* **2015**, C71, 3–8.
- (21) Wolff, S. K.; Grimwood, D. J.; McKinnon, J. J.; Turner, M. J.; Jayatilaka, D.; Spackman, M. A. Crystal Explorer ver. 3.1. University of Western Australia, Perth, Australia **2013**.
- (22) Yang, S. S.; Bai, Y. L.; Xing, F. F.; Zhao, Y. M.; Li, M. X.; Shao, M.; Zhu, S. R. Structural diversity and magnetic properties of six metal organic coordination polymers based on semi-rigid V-shape tetracarboxylic acid ligand. *J. Mol. Struct.* **2016**, 1109, 161–170.
- (23) Goswami, S.; Leitus, G.; Tripuramallu, B. K.; Goldberg, I. Mn^{II} and Co^{II} coordination polymers showing field-dependent magnetism and slow magnetic relaxation behavior. *Cryst. Growth Des.* **2017**, 17, 4393–4404.
- (24) Chen, M.; Chen, S. S.; Okamura, T.; Su, Z.; Chen, M. S.; Zhao, Y.; Sun, W. Y.; Ueyama, N. pH dependent structural diversity of metal complexes with 5-(4H-1,2,4-triazol-4-yl)benzene-1,3-dicarboxylic acid. *Cryst. Growth Des.* **2011**, 11, 1901–1912.
- (25) Montazerzohori, M.; Masoudiasl, A.; Doert, T.; Seykens, H. Structural and computational study of some new nano-structured Hg(II) compounds: a combined X-ray, Hirshfeld surface and NBO analyses. *RSC Adv.* **2016**, 6, 21396–21412.